Aerosol effects on stratocumulus water paths in a PDF-based parameterization

H. Guo,[1] J.-C. Golaz,[2] and L. J. Donner[2]

Received 21 June 2011; revised 8 August 2011; accepted 12 August 2011; published 10 September 2011.

[1] Successful simulation of aerosol indirect effects in climate models requires parameterizations that capture the full range of cloud-aerosol interactions, including positive and negative liquid water path (LWP) responses to increasing aerosol concentrations, as suggested by large eddy simulations (LESs). A parameterization based on multi-variate probability density functions with dynamics (MVD PDFs) has been incorporated into the single-column version of GFDL AM3, extended to treat aerosol activation, and coupled with a two-moment microphysics scheme. We use it to explore cloud-aerosol interactions. In agreement with LESs, our single-column simulations produce both positive and negative LWP responses to increasing aerosol concentrations, depending on precipitation and free atmosphere relative humidity. We have conducted sensitivity tests to vertical resolution and droplet sedimentation parameterization. The dependence of sedimentation on cloud droplet size is essential to capture the full LWP responses to aerosols. Further analyses reveal that the MVD PDFs are able to represent changes in buoyancy profiles induced by sedimentation as well as enhanced entrainment efficiency with aerosols comparable to LESs. **Citation:** Guo, H., J.-C. Golaz, and L. J. Donner (2011), Aerosol effects on stratocumulus water paths in a PDF-based parameterization, *Geophys. Res. Lett.*, *38*, L17808, doi:10.1029/2011GL048611.

1. Introduction

[2] Cloud-aerosol interaction is a major source of uncertainty in climate models [e.g., *Intergovernmental Panel on Climate Change*, 2007]. Many state-of-the-art General Circulation Models (GCMs) include some representation of cloud-aerosol interactions (aerosol indirect effects). However, compared to inverse calculations and satellite estimates, GCMs likely overestimate the magnitude of aerosol indirect effects [e.g., *Lohmann and Lesins*, 2002; *Anderson et al.*, 2003]. A recent GCM intercomparison showed that most GCMs overestimate the positive relationship between aerosol optical depth and liquid water path (LWP) by more than a factor of two [*Quaas et al.*, 2009]. The magnitude of the GCM simulated indirect effects has also been found to be sensitive to formulation details. For example, a threshold value for the conversion from cloud water to rain can result in a ±50% change in the anthropogenic radiative flux perturbation [*Golaz et al.*, 2011], and an unphysical constraint on minimum cloud droplet number concentration reduces the indirect effects by up to 80% [*Hoose et al.*, 2009].

[3] *Ackerman et al.* [2004] showed that liquid water paths can either increase or decrease in response to increasing aerosol concentrations. Using large eddy simulations (LESs) of stratocumulus clouds, they demonstrated that an increase in aerosol concentration reduces cloud water sedimentation and increases cloud-top entrainment. Enhanced entrainment can lead to either an increase or a decrease in LWP depending on the free atmosphere relative humidity. In case of a decrease in LWP, the magnitude of the indirect effects is reduced. Most GCMs cannot capture this negative LWP response to aerosols, partly because they do not incorporate the effect of cloud droplet size on sedimentation and entrainment. It is plausible that neglecting this effect may partially account for the overestimation of the magnitude of the indirect effects in GCMs.

[4] We investigate whether a new class of boundary layer cloud parameterization, based on multi-variate probability density functions with dynamics (MVD PDFs), is able to capture this effect. The MVD PDFs represent the subgrid variations in vertical velocity, liquid water potential temperature, and total water content in a model grid box [*Larson et al.*, 2002; *Golaz et al.*, 2002a, 2002b]. The inclusion of vertical velocity can not only predict subgrid variations in vertical velocity required by aerosol activation, but also combine dynamic and thermodynamic variabilities in a self-consistent framework. The MVD PDFs have been extended to treat aerosol activation and to predict cloud droplet number concentrations, coupled with a two-moment microphysics scheme [*Guo et al.*, 2010, and references therein], and incorporated in the single-column model (SCM) version of the GFDL GCM AM3 [*Donner et al.*, 2011]. The main purpose of this work is to explore whether the MVD PDFs can capture both positive and negative LWP responses to increasing aerosols for boundary layer clouds, as suggested by LESs. And if this is the case, are the underlying physical mechanisms similar?

2. Stratocumulus Case Studies

[5] We use the single-column model described by *Guo et al.* [2010]. It consists of a cloud and turbulence parameterization referred to as CLUBB (Cloud Layers Unified By Binormals) [*Larson and Golaz*, 2005; *Golaz et al.*, 2007], which is based on the MVD PDFs methodology. It is coupled to an aerosol activation scheme [*Ming et al.*, 2006] and the GFDL implementation of the Morrison-Gettelman (MG) two-moment microphysics [*Morrison and Gettelman*, 2008; *Salzmann et al.*, 2010]. We note that CLUBB does not include an explicit entrainment parameterization as is often the case

[1]UCAR Visiting Scientist Programs, Geophysical Fluid Dynamics Laboratory, NOAA, Princeton, New Jersey, USA.
[2]Geophysical Fluid Dynamics Laboratory, NOAA, Princeton, New Jersey, USA.

0094-8276/11/2011GL048611

Table 1. Single-Column Model Configurations

	Resolution		Sedimentation		LWP Response of Both Signs (Yes/No)
	Δz (m)	Δt (min.)	On/Off	Dependence	
Base	5	0.5	on	mass, number	Y
Sensitivity					
resolution	10	1	on	mass, number	Y
	20	1	on	mass, number	Y
	40	3	on	mass, number	Y
sedimentation	5	0.5	off		N
	5	0.5	on	mass	N

in GCMs. Instead, CLUBB predicts vertical profiles of turbulence fluxes, and these fluxes control the entrainment rate. This approach is analogous to the representation of entrainment in LES.

[6] The simulations presented here are based on three nocturnal marine cases studied by the Global Energy and Water Exchange Cloud System Study (GCSS) Boundary Layer Cloud Working Group:

[7] 1. A drizzling stratocumulus case from the Atlantic Stratocumulus Transition Experiment (ASTEX) over the northeastern Atlantic [*Bretherton et al.*, 1995].

[8] 2. A non-drizzling stratocumulus case from the First Research Flight (RF01) of the Second Dynamics and Chemistry of Marine Stratocumulus Field Study (DYCOMS-II) to the west-southwest of San Diego, California [*Stevens et al.*, 2005].

[9] 3. A drizzling stratocumulus case from the Second Research Flight (RF02) of DYCOMS-II [*Ackerman et al.*, 2009].

[10] Our single-column simulations are subject to the same initial conditions and large-scale forcings as the GCSS LES [*Stevens et al.*, 2005; *Ackerman et al.*, 2009]. Longwave radiative fluxes are calculated online using the idealized parameterization from *Stevens et al.* [2005], which does not depend on cloud droplet size distributions. The free atmosphere relative humidities for ASTEX, RF01, and RF02 are ~70%, 10%, and 20%, respectively. To explore the impact of the free atmosphere relative humidity on LWP, *Ackerman et al.* [2004] conducted an additional test with a reduced relative humidity for ASTEX, referred to as 'dry ASTEX'. Here we also add this 'dry ASTEX' case with a free atmosphere relative humidity of ~25%. Simulations are run for 8 hours. In order to better resolve the inversion, we use a vertical spacing (Δz) of ~5 m in the lowest 2 km and a time step (Δt) of 0.5 min in the base configuration (Table 1). The vertical resolution is comparable to those used in LESs [*Stevens et al.*, 2005]. The sensitivity to resolution is discussed below.

[11] As emphasized by *Ackerman et al.* [2004, 2009], cloud water sedimentation plays an essential role in cloud top entrainment (drying) and impacts the responses of LWP to aerosols. In the MG microphysics, terminal velocities for cloud droplet mass and number are obtained by integrating over particle size distributions [*Morrison and Gettelman*, 2008, equations 17 and 18]. Note that the dependence of terminal velocities on droplet number concentration differs in two-moment microphysics (like MG) and one-moment microphysics. We will examine the consequences of this difference in Section 3.

3. Results

[12] To explore the relationship between aerosols and clouds, we perform a number of SCM experiments in which both aerosol mass and number concentrations are progressively increased through fixed aerosol size distributions, which causes cloud droplet number concentration (N_d) to increase. Figure 1 shows LWP, surface precipitation rate, and cloud top entrainment rate (w_e) as a function of N_d for ASTEX, dry ASTEX, RF01, and RF02, as well as the comparisons with LESs from *Ackerman et al.* [2004]. Note that the LES comparison for RF02 is unavailable. To facilitate the comparison with *Ackerman et al.* [2004], LWP and precipitation rate are averaged over 6–8 hours and w_e is averaged over 0–8 hours. w_e is the sum of large-scale subsidence and rate of increase of inversion height [*Stevens et al.*, 2003].

[13] SCM results (Figures 1a and 1b) show that when precipitation is large (>0.1 mm day^{-1}), LWP increases with N_d (or aerosols), consistent with the second aerosol indirect effect hypothesis [*Albrecht*, 1989]. When precipitation is small, the responses of the LWP to increasing aerosol concentrations are positive for ASTEX but negative for dry ASTEX, RF01, and RF02. LWP increases with N_d over a full range from ~30 to 350 cm^{-3} for ASTEX. But for dry

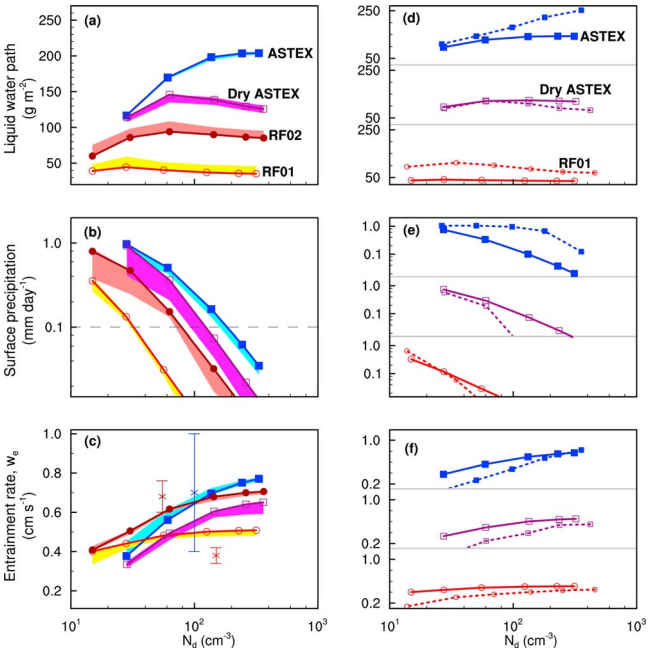

Figure 1. (a) Liquid water path (LWP), (b) surface precipitation rate, and (c) cloud top entrainment rate (w_e) as a function of cloud droplet number concentrations (N_d) from the MVD PDFs simulations. Shaded areas indicate ranges for different vertical resolutions (5 to 40 m) and time steps (0.5 to 3 min). '*' and vertical bars in Figure 1c indicate measurement estimates and ranges of w_e for ASTEX (Blue), RF01 (Red), and RF02 (Dark Red). (d, e, f) Comparisons of the MVD PDFs (solid curves) with LESs conducted by *Ackerman et al.* [2004] (dashed curves).

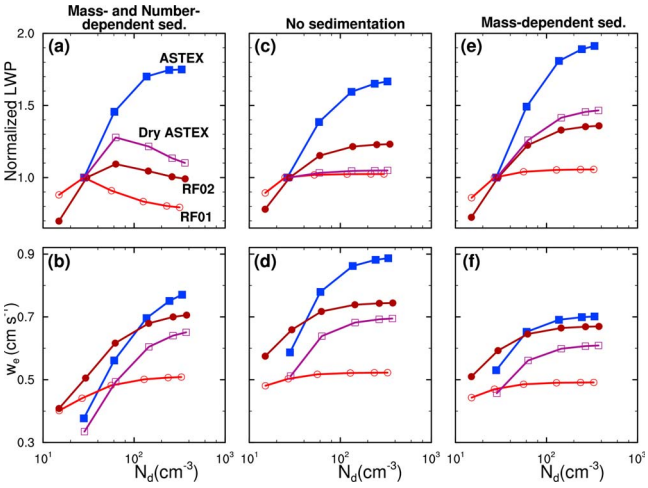

Figure 2. Normalized liquid water path ($\frac{\mathrm{LWP(N_d)}}{\mathrm{LWP(N_d \approx 30\ cm^{-3})}}$) and cloud top entrainment rate (w_e) with (a, b) mass- and number-dependent sedimentation, (c, d) with droplet sedimentation completely omitted, and (e, f) with sedimentation dependent on mass only.

ASTEX, RF01, and RF02, the increases of LWP only occur for N_d less than 60 cm^{-3}, 30 cm^{-3}, and 60 cm^{-3}, respectively. Our SCM results compare favorably with LESs (Figure 1d). The MVD PDFs are capable of capturing a sign reversal in LWP responses with increasing aerosols from positive to negative.

[14] Other responses to aerosols are monotonic. Precipitation decreases and entrainment increases for both SCM and LES (Figures 1b, 1c, 1e, and 1f). The simulated entrainment rate (w_e) also agrees well with measurements for ASTEX and RF02 (vertical bars in Figure 1c). But for RF01, the MVD PDFs overestimate w_e as do most LESs [*Stevens et al.*, 2005].

[15] These results can be explained as follows. The response of LWP to aerosols is largely determined by two competing processes: precipitation and entrainment. Higher aerosol concentrations suppress precipitation but enhance entrainment (Figures 1b, 1c, 1e, and 1f). The suppression of precipitation increases LWP, while the enhancement of entrainment decreases LWP if the entrained air is sufficiently dry. Only when the precipitation dominates the entrainment does LWP increase with aerosols. Otherwise, LWP can either increase or decrease with aerosols depending on whether the entrained air is sufficiently dry.

[16] Simulations of stratocumulus under inversions are often sensitive to model resolution [*Stevens et al.*, 1999]. To test the robustness of our results, we perform sensitivity tests with vertical resolution varying from 5 to 40 m and time step from 0.5 to 3 min (Table 1). Shaded areas in Figures 1a–1c illustrate the range of results. It is clear that these tests converge well. The responses of LWP, precipitation, and w_e to aerosols are consistent across simulations. The convergence and consistency provide confidence in the robustness of the MVD PDFs methodology, and corroborate our findings of positive and negative LWP responses, monotonic decrease of precipitation, and monotonic increase of entrainment as aerosol concentration increases.

[17] *Ackerman et al.* [2004], *Bretherton et al.* [2007], and *Ackerman et al.* [2009] emphasized the role of cloud water sedimentation for properly capturing entrainment. Sedimentation can suppress entrainment by moving cloud water downward, reducing the amount of water available for both entrainment-induced evaporative cooling and cloud-top radiative cooling, and thus diminishing turbulence generation. Therefore, sedimentation imposes a subtle but profound effect on the LWP responses via entrainment.

[18] To test whether a similar response of LWP can be found in our SCM, we perform two series of additional sensitivity experiments (Table 1) in which: (1) cloud water sedimentation is completely omitted; and (2) sedimentation depends only on mass by assuming a constant in-cloud droplet number concentration of 100 cm^{-3} only for computing sedimentation velocities. The latter experiment is conceptually similar to one-moment microphysics schemes. Our purpose is to pinpoint what specific aspects of sedimentation are necessary for the sign reversal in LWP response to increasing aerosols.

[19] Figure 2c shows the normalized LWP when cloud water sedimentation is omitted. In contrast to Figure 2a in which sedimentation depends on both cloud droplet mass and number, LWP increases and eventually reaches a plateau for dry ASTEX, RF01, and RF02. The entrainment rate w_e increases with N_d and is enhanced because more water is available for entrainment drying and cloud-top radiative cooling due to the suppression of sedimentation. But the enhancement of entrainment with N_d is less noticeable, i.e., the omission of cloud water sedimentation reduces the difference of entrainment across the range of N_d (Figures 2b and 2d). This diminishes the dependence of entrainment on N_d. Since the entrainment loses its leverage, the suppression of precipitation by N_d (or aerosols) leads to a higher LWP (Figure 2c).

[20] Similarly, a sedimentation dependent on mass only diminishes the variation in entrainment with N_d (Figure 2f). LWP increases with N_d (Figure 2e). Either mass-only dependent sedimentation or omission of sedimentation reduces the dependence of entrainment on N_d or aerosols (Figures 2d and 2f). The enhancement in entrainment is dominated by the reduction in precipitation, leading to an enhancement in LWP as the aerosol concentration increases (Figures 2c and 2e). This suggests that a more realistic mass- and number-dependent sedimentation scheme is required to reveal the difference in entrainment with aerosols and to capture both positive and negative responses in LWP. The failure of the LWP to decrease in dry ASTEX, RF01, and RF02 when sedimentation does not depend on droplet size suggests the use of one-moment microphysics parameterizations is qualitatively problematic in representing indirect effects depending on sedimentation and entrainment.

4. Buoyancy and Entrainment Efficiency

[21] To further clarify the physical mechanisms of the non-monotonic LWP responses to increasing aerosols with the MVD PDFs, we analyzed buoyancy flux ($\overline{w'b'}$, $\overline{w'b'} = g\frac{\overline{w'\theta_v'}}{\theta_{ref}}$, where θ_v' is virtual potential temperature perturbation, θ_{ref} is a reference temperature of 300.0 K, and g is gravity). Figures 3a–3d show the averaged profiles over 6–8 hours at a high N_d (~350 cm^{-3}) corresponding to a low sedimentation rate (Low Sed., solid curve), and at a low N_d (~30 cm^{-3}, High Sed., dotted curve). The sedimentation rate can differ

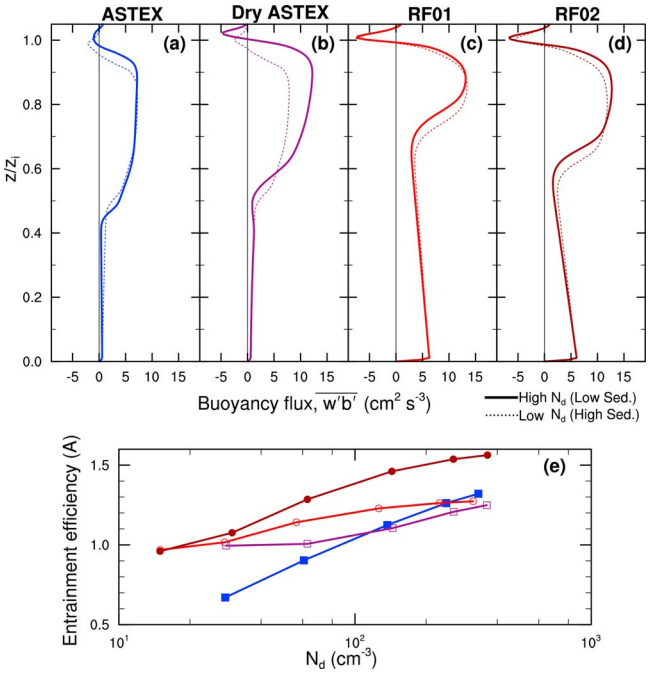

Figure 3. (a-d) Buoyancy flux as a function of normalized height for a high N_d ($N_d \approx 350$ cm^{-3}, or low cloud droplet sedimentation rate; solid curves) and a low N_d ($N_d \approx 30$ cm^{-3}, or high droplet sedimentation; dotted curves). (e) Nondimensional entrainment efficiency (A) as a function of N_d.

roughly by a factor of 3 between the Low Sed. and High Sed. simulations.

[22] *Bretherton et al.* [2007, Figure 1b] analyzed LESs of DYCOMS-II RF01. They showed that sedimentation slightly decreases the buoyancy flux in upper cloud layers, and thus reduces entrainment. Our SCM captures the same response (Figure 3c): a decrease in buoyancy in the upper cloud layers ($0.9 < z/z_i < 1.0$, where z_i is inversion height). The fact that the buoyancy flux response is similar between LESs and SCM gives us further confidence that the MVD PDFs are able to capture the underlying physical mechanisms linking sedimentation and entrainment.

[23] Other cases show qualitatively similar responses of the buoyancy to sedimentation (Figures 3a, 3b, and 3d). However, the quantitative response varies, largely due to different meteorological conditions. For example, dry ASTEX exhibits a much larger buoyancy change between Low Sed. and High Sed. simulations than ASTEX does.

[24] The entrainment rate, w_e, is affected not only by the sedimentation but also by the meteorological conditions such as inversion properties. For example, w_e varies appreciably from 0.4 to 0.8 cm s^{-1} for ASTEX but only slightly from 0.4 to 0.5 cm s^{-1} for RF01 (Figure 1c). *Bretherton et al.* [2007] discuss a nondimensional entrainment efficiency A ($A = w_e \Delta b\, z_i w_*^{-3}$), where Δb ($\Delta b = g\frac{\Delta\theta_v}{\theta_{ref}}$) is the virtual temperature jump ($\Delta\theta_v$) scaled into a buoyancy jump, and w_* is a convective velocity ($w_* = (2.5\int_0^\infty \overline{w'b'}dz)^{1/3}$). Figure 3e shows A as a function of N_d for our base tests. As expected, A decreases with sedimentation (or smaller N_d). A is approximately an exponentially increasing function of N_d. Furthermore, the spread in A for different cases (e.g., ASTEX and RF01) is smaller than that in w_e (Figure 1c), thus better isolating the impact of N_d on A.

5. Concluding Remarks

[25] Single-column simulations with the MVD PDFs are able to represent both positive and negative LWP responses to increasing aerosols, consistent with LES studies [*Ackerman et al.*, 2004]. With higher aerosol concentrations, precipitation is reduced and entrainment is enhanced, but LWP can be either increased or reduced. LWP generally increases with aerosols, when precipitation is a dominant sink of cloud water (>0.1 mm day^{-1}). On the contrary, when the precipitation is weak and the air above clouds is dry, LWP decreases with increasing aerosols.

[26] Analysis of buoyancy flux profiles reveals that sedimentation reduces buoyancy near the inversion and suppresses cloud-top entrainment, similarly to LESs. A mass- and number-dependent droplet sedimentation scheme can capture the effect of cloud droplet number on sedimentation and simulate both positive and negative LWP responses to increasing aerosols. However, either the omission of cloud droplet sedimentation or a sedimentation dependent on mass only (as adopted in one-moment microphysics) fails to capture the negative LWP response. This failure could potentially amplify the increase of LWP with aerosols and overestimate the magnitude of the aerosol indirect effects.

[27] The impacts of droplet size distributions on microphysics and radiation have not been considered here. Aerosol-related changes in droplet size distributions could impact entrainment by modifying cloud condensation and evaporation, and impose another aerosol indirect effect [*Liu and Daum*, 2002; *Wang et al.*, 2003; *Xue and Feingold*, 2006].

[28] Successful single-column simulations suggest that the MVD PDFs are able to capture a wide range of the aerosol indirect effects in a manner consistent with LESs. The entrainment rate in the MVD PDFs is controlled by the prognostic turbulence fluxes. Through the ability of the MVD PDFs to simulate negative responses of LWP to aerosols, it is conceivable that the use of MVD PDFs in GCMs could lower the magnitude of the simulated indirect effects and thus help reconcile GCMs with satellite or inverse estimates. In a full GCM, the goal will be to use MVD PDFs as a comprehensive parameterization for boundary layers, associated shallow cumulus and stratocumulus, and aerosol interactions with boundary layer clouds. GCM implementation will raise issues of generality over a considerably wider range of synoptic situations [*Guo et al.*, 2010] and the extent to which vertical resolution and time step can be relaxed to meet computational limitations.

[29] **Acknowledgments.** H. Guo is supported by the NOAA Climate Program Office through the Climate Process Team, Cloud Macrophysical Parameterization and its Application to Aerosol Indirect Effects. We acknowledge Vincent E. Larson and his group for their continued support of the CLUBB parameterization. We thank Hugh Morrison and Andrew Gettelman for their two-moment microphysics source code. We also thank Andrew S. Ackerman for kindly providing datasets of LES results in electronic form.

[30] The Editor thanks two anonymous reviewers for their assistance in evaluating this paper.

References

Ackerman, A. S., M. P. Kirkpatrick, D. E. Stevens, and O. B. Toon (2004), The impact of humidity above stratiform clouds on indirect aerosol climate forcing, *Nature*, *432*, 1014–1017.

Ackerman, A. S., et al. (2009), Large-eddy simulations of a drizzling, stratocumulus-topped marine boundary layer, *Mon. Weather Rev.*, *137*(3), 1083–1110, doi:10.1175/2008MWR2582.1.

Albrecht, B. A. (1989), Aerosols, cloud microphysics, and fractional cloudiness, *Science*, *245*, 1227–1230.

Anderson, T. L., R. J. Charlson, S. E. S. R. Knutti, O. Boucher, H. Rodhe, and J. Heintzenberg (2003), Climate forcing by aerosols—A hazy picture, *Science*, *300*, 1103–1104, doi:10.1126/science.1084777.

Bretherton, C. S., P. Austin, and S. T. Siems (1995), Cloudiness and marine boundary layer dynamics in the ASTEX Lagrangian experiments. Part II: Cloudiness, drizzle, fluxes, and entrainment, *J. Atmos. Sci.*, *52*(16), 2724–2735.

Bretherton, C. S., P. N. Blossey, and J. Uchida (2007), Cloud droplet sedimentation, entrainment efficiency, and subtropical stratocumulus albedo, *Geophys. Res. Lett.*, *34*, L03813, doi:10.1029/2006GL027648.

Donner, L. J., et al. (2011), The dynamical core, physical parameterizations, and basic simulation characteristics of the atmospheric component of the GFDL Global Coupled Model CM3, *J. Clim.*, *24*, 3484–3519, doi:10.1175/2011JCLI3955.1.

Golaz, J.-C., V. E. Larson, and W. R. Cotton (2002a), A PDF-based model for boundary layer clouds. Part I: Method and model description, *J. Atmos. Sci.*, *59*(24), 3540–3551.

Golaz, J.-C., V. E. Larson, and W. R. Cotton (2002b), A PDF-based model for boundary layer clouds. Part II: Model results, *J. Atmos. Sci.*, *59*(24), 3552–3571.

Golaz, J.-C., V. E. Larson, J. A. Hansen, D. P. Schanen, and B. M. Griffin (2007), Elucidating model inadequacies in a cloud parameterization by use of an ensemble-based calibration framework, *Mon. Weather Rev.*, *135*(12), 4077–4096, doi:10.1175/2007MWR2008.1.

Golaz, J.-C., M. Salzmann, L. J. Donner, L. W. Horowitz, Y. Ming, and M. Zhao (2011), Sensitivity of the aerosol indirect effect to subgrid variability in the cloud parameterization of the GFDL Atmosphere General Circulation Model AM3, *J. Clim.*, *24*, 3145–3160, doi:10.1175/2010JCLI3945.1.

Guo, H., J.-C. Golaz, L. J. Donner, V. E. Larson, D. P. Schanen, and B. M. Griffin (2010), Multi-variate probability density functions with dynamics for cloud droplet activation in large-scale models: Single column tests, *Geosci. Model Dev.*, *3*, 475–486, doi:10.5194/gmd-3-475-2010.

Hoose, C., J. E. Kristjánsson, T. Iversen, A. Kirkevåg, Ø. Seland, and A. Gettelman (2009), Constraining cloud droplet number concentration in GCMs suppresses the aerosol indirect effect, *Geophys. Res. Lett.*, *36*, L12807, doi:10.1029/2009GL038568.

Intergovernmental Panel on Climate Change (2007), *Climate Change* 2007*: The Physical Science Basis. Contribution of Working Group I to the Fourth Assessment Report of the Intergovernmental Panel on Climate Change*, edited by S. Solomon et al., 996 pp., Cambridge Univ. Press, Cambridge, U. K.

Larson, V. E., and J.-C. Golaz (2005), Using probability density functions to derive consistent closure relationships among higher-order moments, *Mon. Weather Rev.*, *133*(4), 1023–1042.

Larson, V. E., J.-C. Golaz, and W. R. Cotton (2002), Small-scale and mesoscale variability in cloudy boundary layers: Joint probability density functions, *J. Atmos. Sci.*, *59*(24), 3519–3539.

Liu, Y., and P. H. Daum (2002), Indirect warming effect from dispersion forcing, *Nature*, *419*, 580–581.

Lohmann, U., and G. Lesins (2002), Stronger constraints on the anthropogenic indirect aerosol effect, *Science*, *289*, 1012–1025, doi:10.1126/science.1075405.

Ming, Y., V. Ramaswamy, L. J. Donner, and V. T. J. Phillips (2006), A new parameterization of cloud droplet activation applicable to General Circulation Models, *J. Atmos. Sci.*, *63*(4), 1348–1356, doi:10.1175/JAS3686.1.

Morrison, H., and A. Gettelman (2008), A new two-moment bulk stratiform cloud microphysics scheme in the Community Atmosphere Model, version 3 (CAM3). Part I: Description and numerical tests, *J. Clim.*, *21*, 3642–3659, doi:10.1175/2008JCLI2105.1.

Quaas, J., et al. (2009), Aerosol indirect effects—General circulation model intercomparison and evaluation with satellite data, *Atmos. Chem. Phys.*, *9*, 8697–8717, doi:10.5194/acp-9-8697-2009.

Salzmann, M., Y. Ming, J.-C. Golaz, P. A. Ginoux, H. Morrisson, A. Gettelman, M. Krämer, and L. J. Donner (2010), Two-moment bulk stratiform cloud microphysics in the GFDL AM3 GCM: Description, evaluation, and sensitivity tests, *Atmos. Chem. Phys.*, *10*, 8037–8064, doi:10.5194/acp-10-8037-2010.

Stevens, B., C.-H. Moeng, and P. P. Sullivan (1999), Large-eddy simulations of radiatively driven convection: Sensitivities to the representation of small scales, *J. Atmos. Sci.*, *56*(23), 3963–3984.

Stevens, B., et al. (2003), Dynamics and chemistry of marine stratocumulus DYCOMS-II, *Bull. Am. Meteorol. Soc.*, *84*(5), 579–593.

Stevens, B., et al. (2005), Evaluation of large-eddy simulations via observations of nocturnal marine stratocumulus, *Mon. Weather Rev.*, *133*(6), 1443–1462.

Wang, S., Q. Wang, and G. Feingold (2003), Turbulence, condensation, and liquid water transport in numerically simulated nonprecipitating stratocumulus clouds, *J. Atmos. Sci.*, *60*(2), 262–278.

Xue, H., and G. Feingold (2006), Large eddy simulations of trade wind cumuli: Investigation of aerosol indirect effects, *J. Atmos. Sci.*, *63*(6), 1605–1622.

L. J. Donner and J.-C. Golaz, Geophysical Fluid Dynamics Laboratory, NOAA, Princeton, NJ 08540, USA. (leo.j.donner@noaa.gov; chris.golaz@noaa.gov)

H. Guo, UCAR Visiting Scientist Programs, Geophysical Fluid Dynamics Laboratory, NOAA, Princeton, NJ 08540, USA. (huan.guo@noaa.gov)